Article

Journal of
Nanoscience and Nanotechnology
Vol. 15, 1–11, 2015
www.aspbs.com/jnn

Paclitaxel-Loaded TPGS-*b*-PCL Nanoparticles: *In Vitro* Cytotoxicity and Cellular Uptake in MCF-7 and MDA-MB-231 Cells versus mPEG-*b*-PCL Nanoparticles and Abraxane®

Ezequiel Bernabeu[1,3], Lorena Gonzalez[2,3], Maria J. Legaspi[1], Marcela A. Moretton[1,3], and Diego A. Chiappetta[1,3,*]

[1] *Department of Pharmaceutical Technology, Faculty of Pharmacy and Biochemistry, University of Buenos Aires, Buenos Aires CP1113, Argentina*
[2] *Department of Biological Chemistry, Faculty of Pharmacy and Biochemistry, University of Buenos Aires, Argentina*
[3] *National Science Research Council (CONICET)*

Nanomedicines have become an attractive platform for the development of novel drug delivery systems in cancer chemotherapy. Polymeric nanoparticles (NPs) represent one of the best well-investigated nanosized carriers for delivery of antineoplastic compounds. The "Pegylation strategy" of drug delivery systems has been used in order to improve carrier biodistribution, however, some nanosized systems with PEG on their surface have exhibited poorly-cellular drug internalization. In this context, the purpose of the present study was to compare *in vitro* performance of two paclitaxel (PTX)-loaded NPs systems based on two biocompatible copolymers of alpha tocopheryl polyethylene glycol 1000 succinate-*block*-poly(ε-caprolactone) (TPGS-*b*-PCL) and methoxyPEG-*block*-poly(ε-caprolactone) (mPEG-*b*-PCL) in terms of citotoxicity and PTX cellular uptake. Furthermore, TPGS-*b*-PCL NPs were also copared with the commercially available PTX nano-sized formulation Abraxane®. Both TPGS-*b*-PCL and mPEG-*b*-PCL derivates were synthesized by ring opening polymerization of ε-caprolactone employing microwaved radiation. NPs were obtained by a solvent evaporation technique where the PTX content was determined by reverse-phase HPLC. The resulting NPs had an average size between 200 and 300 nm with a narrow size distribution. Also both NPs systems showed a spherical shape. The *in vitro* PTX release profile from the NPs was characterized employing the dialysis membrane method where all drug-loaded formulations showed a sustained and slow release of PTX. Finally, *in vitro* assays demonstrated that PTX-loaded TPGS-*b*-PCL exhibited a significant higher antitumor activity than PTX-loaded mPEG-*b*-PCL NPs and Abraxane® against an estrogen-dependent (MCF-7) and an estrogen independent (MDA-MB-231) breast cancer cells lines. Furthermore TPGS-*b*-PCL NPs showed a significant increase on PTX cellular uptake, for both breast cell lines, in comparison with mPEG-*b*-PCL NPs and Abraxane®. Overall findings confirmed that NPs based on TPGS-*b*-PCL as biomaterial demonstrated a better *in vitro* performance than NPs with PEG, representing an attractive alternative for the development of novel nanosized carriers for anticancer therapy.

Keywords: TPGS-*b*-PCL Polymeric Nanoparticles, Paclitaxel, *In Vitro* Anti-Tumoral Activity, Cellular Uptake.

1. INTRODUCTION

In recent years, novel anti-cancer therapy strategies based in nanomedicines have become an attractive platform in drug delivery systems.[1–3] Nanosized carriers exhibits countless advantages, some of them related with (i) improved drug aqueous solubility, chemical stability, efficacy and safety, (ii) prolonged drug biodistribution after an intravenous administration, (iii) reduced side

*Author to whom correspondence should be addressed.

effects and, (iv) sustained drug release, (v) passive drug targeting due to the extravasations of polymers and nanosized system from tumor blood vessels and their retention in tumor tissues (Enhanced Permeability and Retention (EPR) effect) and (vi) active drug targeting.[4–6] Particularly, polymeric nanoparticles (NPs) development based on biocompatible polymers for antineoplastic drug delivery has attracted much interest for novel cancer chemotherapy.[7, 8] Initially, hydrophobic polymers were the most employed NPs-former biomaterials. However, these NPs systems denoted the rapid blood clearance by the reticuloendothelial system (RES), leading to inefficient EPR effect after intravenous injection. To overcome this drawback, the NPs were modified in their surface with hydrophilic materials that could prevent NPs premature blood clearance, favoring its preferential accumulation in solid tumors by EPR effect.[9]

Among various FDA approved polymers, the biocompatible and biodegradable poly(ε-caprolactone) (PCL) has been widely studied to prepare NPs for pharmaceutical applications.[10] However, its hydrophobic nature along with its slow degradation rate and the fast PCL NPs uptake by the RES, make them inappropriate for intravenous drug delivery systems.[11] In an attempt to overcome these issues, PCL copolymerization with others monomers was investigated. Therefore, NPs based on copolymers with a suitable hydrophobic–hydrophilic balance could reduce the addition of blood proteins and modify the matrix degradation rates.[12] It has been widely studied the copolymerization of PCL with polyethylene-glycol (PEG),[13–15] where the hydrophilic nature of the NPs surface avoid recognition by RES improving NPs circulation time in blood.[9] Although this surface "PEGylation strategy" has been demonstrated to improve the pharmacokinetics and biodistribution of a different antineoplastic compounds,[16] some drug delivery "nanosized" systems with PEG on their surface present poorly-cellular drug internalization,[17, 18] which results in significant loss of activity of the delivery system. In this context, the study of other hydrophilic materials that could replace PEG represents a pending agenda that must be resolved for antineoplastic chemotherapy. A simple strategy would be to use PEG derivatives that can improve the cellular uptake without losing the biodistribution and pharmacokinetics of PEG.

One surfactant used recently for surface coating is the D-α-tocopheryl polyethylene glycol 1000 succinate (vitamin E TPGS or TPGS), which is a water-soluble derivative of natural source vitamin E and PEG.[19] It is a biocompatible, non-ionic surfactant which has been widely applied in pharmaceutical formulations because it could enhance the solubility and bioavailability of some poorly absorbed drugs.[20, 21] Furthermore, TPGS can be used in NPs formulations, where it acts as an emulsifier or coating material to improve encapsulation efficiency and cellular uptake.[22] TPGS has potential effects for cancer chemotherapy since it could inhibit the P glycoprotein (P-gp) known as an efflux pump which mediates multidrug resistance in tumor cells. Thereafter TPGS could enhance anticancer drug permeation.[23] Moreover, it has been reported that TPGS exhibited *in vitro* and *in vivo* antineoplastic activity on different cancer cell lines by promoting cellular apoptosis.[24] Therefore, a biocompatible derivate of D-α-tocopheryl polyethylene glycol 1000 succinate-*block*-poly(ε-caprolactone) (TPGS-*b*-PCL) represents an interesting approach to improve the antineoplastic efficacy of NP formulations.

In this framework, the present study evaluated the *in vitro* performance of anticancer drug paclitaxel (PTX)-loaded TPGS-*b*-PCL NPs versus PTX-loaded methoxy(polyethyleneglycol)-*block*-poly(ε-caprolactone) (mPEG-*b*-PCL) NPs and the drug commercially available nanosized-formulation Abraxane®. Both biocompatible amphiphilic block copolymers were synthesized by ring opening polymerization employing microwave radiation with the same hydrophilic–hydrophobic balance. Then, NPs were obtained by a solvent evaporation technique and characterized in terms of drug loading, size and size distribution and surface morphology. Also the *in vitro* PTX release profile from the NPs was characterized employing the dialysis membrane method. Finally, to determine if PTX-loaded TPGS-*b*-PCL NPs could achieve better performance *in vitro* than mPEG-*b*-PCL NPs and Abraxane®, we report their antitumor activities and PTX cellular uptake against an estrogen-dependent (MCF-7) and an estrogen independent (MDA-MB-231) breast cancer cells lines. Moreover the inhibition of P-gp efflux pumps was assessed for all formulations with and without verapamil.

2. EXPERIMENTAL DETAILS

2.1. Materials

Paclitaxel (PTX) of purity 99.9% was purchased from Rhenochem AG (Switzerland), D-α-tocopheryl polyethylene-glycol 1000 succinate (TPGS, MW ~1513 g/mol) was from Eastman Chemical Company (USA), methoxy(polyethylene glycol) (mPEG, MW~5,000 g/mol), ε-caprolactone (ε-CL, MW 114.14 g/mol), tin(II) 2-ethylhexanoate (SnOct, MW 405.12 g/mol) were purchased from Sigma-Aldrich (USA). Tetrazolium compound [3-(4,5-dimethylthiazol-2-yl)-5-(3-carboxymethoxyphenyl)-2-(4-sulfophenyl)-2H-tetrazolium], inner salt (MTS) and phenazine methosulfate (PMS) were purchased from Promega Corporation (USA). Clinical formulation Abraxane® was supplied by Aventis Pharmaceuticals, USA. All solvents such as acetone, acetonitrile and dichloromethane (DCM) were of analytical or high performance liquid chromatography (HPLC) grade and were used following the manufacturer's instructions.

2.2. Synthesis of mPEG- and TPGS-PCL Copolymer

The copolymer synthesis, for both derivates, was performed as previously described.[25] Briefly, a household

microwave oven (Whirlpool®, WMD20SB, microwave frequency 2450 MHz, potency 800 W, Argentina) with ten power levels was adapted in the laboratory to enable the connection of a condenser. PCL copolymers were synthesized by the ring opening polymerization of ε-CL by mPEG and TPGS for mPEG-*b*-PCL and TPGS-*b*-PCL, respectively; both in presence of SnOct as a catalyst. In the first case, mPEG (0.8 g) was poured into a 250 mL round-bottom flask and dried. Then, ε-CL (12.0 g) and SnOct (0.04 g) were added, and the round-bottom flask was placed in the centre of the microwave oven and connected to the condenser. The reaction mixture was exposed to microwave radiation for:

(i) 1 min at power 4,
(ii) 8 min at power 2 and
(iii) 1 min at power 4.

The total reaction time was 10 min, under reflux. Then, the crude was dissolved in dichloromethane (50 mL) and precipitated in methanol (500 mL) to isolate the product. The product obtained was recuperated by filtration, washed several times with methanol, dried until constant weight at room temperature and stored at 4 °C until use. Finally, a white to yellowish solid was obtained. For the second copolymer (TPGS-*b*-PCL), TPGS (3.0 g) was poured into a 250 mL round-bottom flask and dried. Then, ε-CL (20.0 g) and SnOct (0.04 g) were added, and the round-bottom flask was placed in the centre of the microwave oven and connected to the condenser. In this case, the reaction mixture was exposed to microwave radiation for:

(i) 1 min at power 5,
(ii) 2 min at power 3,
(iii) 2 min at power 3,
(iv) 5 min at power 3 and
(v) 1 min at power 5.

The total reaction time was 11 min, under reflux. Then, the derivate was treated following the same procedure described for mPEG-*b*-PCL synthesis. Finally, a white to yellowish solid was obtained.

Finally the chemical compositions of the mPEG-*b*-PCL and TPGS-*b*-PCL copolymer were determined from proton nuclear magnetic resonance (^{1}H-NMR) spectra in deuterated chloroform (Sigma) at room temperature on a Bruker MSL300 spectrometer (300 MHz, Germany). Number- and weight-average molecular weights (Mn and Mw) and molecular weight distributions (Mw/Mn polydispersity, PDI) were determined by gel permeation chromatography (GPC) using a Knauer GPC instrument (Berlin, Germany) provided with a refractive index detector. A set of 50A, 100A and M2 (Phenomenex Inc., Torrance, CA, USA) and 104A (Waters, Inc., Milford, MA, USA) columns ultrastiragel column, conditioned at 25 °C was used to elute samples at 1mL/min HPLC-grade tetrahydrofuran flow rate. Polystyrene standards (Polymer Laboratories, Shropshire, UK) were used for calibration.

2.3. Preparation of PTX-Loaded NPs

PTX-loaded NPs were prepared using mPEG-*b*- and TPGS-*b*-PCL by a solvent evaporation technique as previously described.[25] First, a stock solution of PTX in dichloromethane (1.4 mg/mL) was prepared. Then, mPEG-*b*- or TPGS-*b*-PCL (42 mg total weight) was added to a 3 mL of PTX stock solution and vortexed until complete dissolution. This solution was poured slowly into distilled water (100 mL) containing TPGS (0.03% w/v) and emulsified by sonication using a probe sonicator (Q700 ultrasonic liquid processor, Qsonica, USA) at an output of 50 W for 60 seconds. The resulting emulsion o/w was stirred under magnetic stirring overnight at room temperature. Then, the sample was vacuum-filtered through filter paper (VWR® Grade 410 Filter Paper, Qualitative, 1 μm) and the suspension was frozen at −20 °C and lyophilized for 48 h employing a freeze-dryer (FIC-L05, FIC, Scientific Instrumental Manufacturing, Argentina) for 48 h. PTX-free NPs were used as controls.

2.4. Determination of PTX Content in NPs

The PTX content was determined by a high performance liquid chromatography (HPLC) where the analytical method was previously validated.[26] Briefly, a reversed phase C18 column (4.6 mm × 250 mm, 5 μm, Fluophase PFP, Thermo, USA) with a mobile phase composed of acetonitrile/water (50/50, v/v) were used. The flow rate was maintained at 1 mL/min and the detection wavelength was 227 nm (UV-detector, Shimadzu SPD-10A, Japan). Sample solutions were injected (Plus autosampler, Shimadzu SIL-10A, Japan) at a volume of 20 μl. The linearity range was establish between 0.05 and 50 μg/mL with standard solutions of PTX dissolved in acetonitrile (correlation coefficient of $R^2 = 0.996$) and the limit of quantification was 0.005 μg/mL. NPs were dissolved in acetonitrile and vigorously vortexed to get a clear solution. Finally, drug loading (DL) and efficiency encapsulation (EE) of drug-loaded NPs were calculated according to Eqs. (1) and (2):

$$\text{DL (\%)} = (\text{Weight of PTX in the NPs} / \text{Total weight of NPs}) \times 100 \quad (1)$$

$$\text{EE (\%)} = (\text{Weight of PTX in NPs} / \text{Initial weight of PTX used}) \times 100 \quad (2)$$

2.5. NPs Characterization

The hydrodynamic diameter (Dh) and polydispersity index (PDI) of PTX-loaded NPs prepared with mPEG-*b*- and TPGS-*b*-PCL copolymers were determined by Dynamic Light Scattering (DLS, Zetasizer Nano-Zs, Malvern Instruments, UK) provided with a He–Ne (633 nm) laser and a digital correlator ZEN3600. Measurements were conducted at a scattering angle of $\theta = 173°$ to the incident beam. Samples were equilibrated at 25 °C for at least 3 min prior to the analysis. Previously, the instrument was

calibrated with standard latex NPs provided by Malvern Instruments (UK). Zeta potential was measured using the same instrument at 25 °C. Experimental values were the average of three different formulations.

The morphology of lyophilized PTX-loaded NPs was characterized by means of Field Emission Gun Scanning Electron Microscopy (FEG-SEM, Zeiss Supra 40 TM apparatus Gemini column, Germany) operating at an accelerating voltage of 3.0 kV. NPs were coated with a thin layer of gold (thickness of 5–10 nm) by sputtering method.

2.6. *In Vitro* PTX Release

In vitro release profiles of PTX from mPEG-*b*-, TPGS-*b*-PCL NPs and Abraxane® were performed using the dialysis method over 96 h. Systems containing 0.5 mg of PTX were dispersed in phosphate buffer USP 30 (pH 7.4, 5 mL) containing 0.5% v/v of polysorbate 80. The resulting suspension was placed into a dialysis bag (regenerated cellulose dialysis membranes; molecular weight cut off of 3500 g/mol; Spectra/Por® 3 nominal flat width of 45 mm, diameter of 29 mm and volume/length ratio of 6.4 mL/cm; Spectrum Laboratories, Inc., USA), sealed, and placed in a Falcon® conical tube (50 mL) containing the release medium (PBS, pH 7.4 containing 0.5% v/v of polysorbate 80, 45 mL). Polysorbate 80 was added to increase the intrinsic solubility of PTX in the release medium and to ensure sink conditions.[27] Then, each Falcon® conical tube was placed in an orbital water bath and maintained at 37.0 ± 0.5 °C with stirring rate of 40 rpm. The release media (45 mL) was sampled at predetermined time intervals (1, 2, 4, 6, 8, 24, 48, 72 and 96 h) and replaced with equal volume of fresh medium pre-heated at 37 °C. The samples were analyzed for PTX content by HPLC as described above (with minor modifications) with correction for the volume replacement. Assays were carried out in triplicate and the results are expressed as mean ± S.D.

2.7. *In Vitro* Cytotoxicity

Human breast cancer cell lines (MCF-7 and MDA-MB 231) were obtained from the American Type Culture Collection (ATCC) (Rockville, MD, USA). Cells were maintained in Dulbecco's minimum essential medium (DMEM®) supplemented with 2 mM L-glutamine (Invitrogen, Argentina), 10% fetal bovine serum (FBS) and 50 μg/mL gentamycine (Invitrogen, Argentina) at 37 °C (humidified atmosphere of 5% CO_2). For *in vitro* cytotoxicity assays, cells were seeded in clear 96-well plates (Corning Costar, Fisher Scientific, USA) at a density of 5,000 cells/well and incubated 24 h to allow cell attachment. Then, cells were incubated with PTX, Abraxane® and PTX-loaded mPEG-*b*-PCL NPs and TPGS-*b*-PCL NPs for 48 and 72 h. The final concentration of PTX was in the range of 0.1 and 50 μg/mL. Drug-free NPs and blank culture medium were used as controls. After the each predetermined incubation period, the medium was removed, the wells were washed with PBS and fresh medium was added. Finally, a solution of water-soluble tetrazolium salts (WST), prepared according to manufactures instructions (CellTiter 96® aqueous non-radioactive cell proliferation assay, Promega), was added and the cells were incubated for 2 h. Finally, absorbance at 490 nm was measured using a microplate reader (Biotrak II Plate Reader, Amershan Bioscienes, Piscataway, New Jersey, USA). PTX concentrations required to inhibit growth by 50% (IC50) were determined from concentration-dependent cell viability curves. Assays were done by triplicate. Values were expressed in terms of percent of untreated control cells set as 100%.

2.8. *In Vitro* Cellular Uptake

To evaluate the cellular uptake of PTX encapsulated within NPs modified with mPEG or TPGS on the particle surface, we determined PTX by HPLC assay of collected MCF-7 and MDA-MB 231 cells, which were incubated with various PTX formulations for different incubation times. Briefly, MCF-7 or MDA-MB231 cells were seeded into 6-well plates at 4×10^5 cells/well and cultured at 37 °C in the presence of 5% CO_2 for 24 h to permit the attachment of cells. The cells were then incubated with PTX, free- and PTX-loaded mPEG-*b*-PCL NPs, and free- and PTX-loaded TPGS-*b*-PCL NPs at 25 μg/mL of PTX for 0.5, 2, 4 and 6 h, respectively. At predetermined time-points, the cells were washed with 1.5 mL ice cold PBS to terminate the uptake and remove the drug or systems that were adsorbed on the cell membrane. Then, the cells were washed with PBS and 0.25 mL trypsin PBS solution (2.5 μg/mL) was added. The cell lysate was centrifuged at 13,000 rpm (MiniSpin® plus™, Eppendorf, Germany) for 10 min. Drug content in the supernatant after centrifugation was measured by HPLC method and obtained values were normalized by protein content in each sample determined using BCA protein assay kit (Pierce Corporation, Beijing local agent, China) according to the manufacturer's protocol. Statistical analysis of intracellular/cell PTX levels as delivered by the different nanocarriers, Abraxane® and the PTX solution at 6 h was performed by one-way ANOVA test and Dunnett's Multiple Comparison *post-hoc* test using GraphPad Prism version 5.02 for Windows (GraphPad Software, USA). Statistical significance was defined as $p < 0.05$. All experiments were repeated in triplicate.

2.9. Inhibition of P-gp Efflux Pumps

To evaluate the effect of systems on P-gp inhibition, the uptakes of different formulations of PTX (25 μg/mL): PTX with and without 100 μM verapamil, PTX-loaded mPEG-*b*-PCL NPs with and without 100 μM verapamil, and PTX-loaded TPGS-*b*-PCL NPs with and without 100 μM verapamil, were tested on MCF-7 and MDA-MB 231 cells. At this concentration, verapamil did not cause

significant cytotoxicity in both cell lines.[28] Then, the cells were incubated with test solutions at 37 °C for 2 h, the test solutions were removed. Subsequently, the cells were washed by 4 °C PBS thrice, and the amount of PTX in both cells lines were assayed by HPLC. Statistical analysis of intracellular/cell PTX levels as delivered by each formulation in absence and presence of verapamil at 2 h was performed by *t*-test using GraphPad Prism version 5.02 for Windows (GraphPad Software, USA). Statistical significance was defined as $p < 0.05$.

3. RESULTS AND DISCUSSION

3.1. Copolymer Synthesis and Characterization

In order to evaluate the *in vitro* performance on nanosized carriers loaded with the antineoplastic poorly-water soluble PTX, we synthesized two copolymers (mPEG-*b*-PCL and TPGS-*b*-PCL) via ring opening polymerization of ε-CL initiated by PEG in presence of SnOct (Fig. 1). The chemical compositions were determined from ^{1}H-RMN spectra by calculating the ratio of the integral peaks areas corresponding to the Ethylene Oxide (EO, repeating units of TPGS or mPEG) from methylene protons at $\delta = 3.6$–3.65 ppm and the CL ε-mehylene protons at $\delta = 4.0$–4.1 ppm. Both amphiphilic derivates presented an identical hydrophobic/hydrophilic balance. The copolymers compositions can be determined as EO:CL = 16:84 (molar ratio). Mn and Mw values were determined by GPC, where the analysis revealed the presence of an unimodal molecular weight distribution. The Mn value of mPEG-*b*- and TPGS-*b*-PCL copolymers was determined to be 14,482 and 12,062 g/mol, respectively; whereas that the Mw resulted be 29,993 and 21,285 g/mol, respectively. These results show a PDI of 2.07 and 1.76, respectively. Results were in good concordance with the theoretical composition.

3.2. Preparation and Characterization of PTX-Loaded Nanoparticles

Both copolymers, mPEG-*b*-PCL and TPGS-*b*-PCL, were used for produce PTX-loaded NPs by a solvent evaporation technique as previously described.[25] The DL (%) content of TPGS-*b*-PCL and mPEG-*b*-PCL NPs was 6.0 and 8.6% w/w, respectively; these values represented an EE (%) of 66.3 and 94.6%, respectively (Table I).

The size and size distribution of the PTX-loaded NPs prepared by both copolymers are presented in Table I. The size of the two NPs formulation was between 240 and 300 nm. This data represents an excellent size range for cellular uptake of nanosized carriers as it has been previously described.[29] Interestingly, the Dh of the PTX-loaded TPGS-*b*-PCL was much smaller than that of the mPEG-*b*-PCL NPs; this result is probably related with the TPGS component of the copolymer since it presents a self-emulsifying function.[20]

Also, PDI values followed a similar trend where the mPEG-*b*-PCL-based NPs exhibited a grater polydispersion than their counterparts prepared with TPGS-*b*-PCL. In this case, NPs prepared with TPGS-*b*-PCL presented a PDI value of 0.25, while mPEG-*b*-PCL NPs showed a value of 0.30 (Table I). This effect could be also attributed to the self-emulsifying effect of TPGS. Another interesting parameter to investigate is the zeta potential of a colloidal dispersion. It is well known that NPs zeta potential is a crucial factor for nanosized carrier stability in suspension due to the electrostatic repulsion between the NPs. In the present study PTX-loaded NPs showed a negative surface charge with zeta potential values of −31.7 mV and −35.5 mV for mPEG-*b*-PCL and TPGS-*b*-PCL, respectively (Table I). This result might be related with the presence of ionized carboxyl groups of the PCL segments.[30] Thereafter, the repulsion among the highly negatively charged NPs provides extra stability. For both

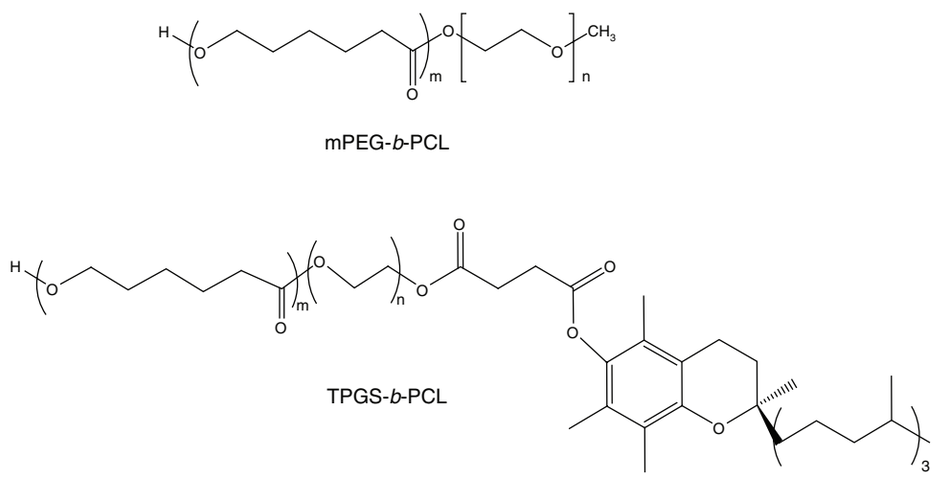

Figure 1. Chemical structures of mPEG-*b*-PCL and TPGS-*b*-PCL.

Table I. PTX payload, encapsulation efficiency, size, size distribution (polydispersity) and zeta potential values of NPs at 25 °C. Results are expressed as mean ± S.D. ($n = 3$).

Copolymer	Size (nm)	Polydispersity	Zeta potential (mV)	Drug loading (% w/w)	Encapsulation efficiency (%)
mPEG-*b*-PCL	303 ± 13	0.30 ± 0.03	−31.7 ± 0.2	8.6 ± 2.2	94.6
TPGS-*b*-PCL	240 ± 10	0.25 ± 0.01	−35.5 ± 1.1	6.0 ± 0.5	66.3

formulations, we did not observe significant changes in the surface charge.

3.3. Morphological Characterization

The surface morphology of the lyophilized PTX-loaded NPs was investigated by means of FEG-SEM. Figure 2 shows the micrographs for PTX-loaded NPs where the mean NPs diameter seemed to be between 200 and 400 nm in diameter and have a spherical shape. In addition, the TPGS-*b*-PCL particles seemed to have smooth surface while mPEG-*b*-PCL NPs showed a rough surface, within SEM resolution level. A similar effect has been previously observed by Zhang et al., where the presence of a hydrophilic material as PEG can create a porous structure in the surface of NPs.[31] Furthermore, NP size estimated from the images is consistent with that obtained by DLS.

3.4. *In Vitro* Release

The *in vitro* cumulative release profiles of PTX from mPEG-*b*-PCL NPs, TPGS-*b*-PCL NPs and Abraxane® are shown in Figure 3. All NPs formulations disclosed a sustained and slow release of PTX, where the amount of drug released in the first 24 h was ∼7%, ∼6% and ∼10% for mPEG-*b*-PCL, TPGS-*b*-PCL and Abraxane®, respectively. After 96 h, the PTX release was ∼19% for mPEG-*b*-PCL, ∼21% for TPGS-*b*-PCL and ∼20% for Abraxane®. As we see in the Figure 3, the release rate was not affected by the type of polymer used in the formulations, and also, none of the formulations showed burst effect. In the case of the NPs, the slow and continuous release may be attributed to the diffusion of the drug localized in the core of the NPs and by the absence of drug absorbed in the surface of the NPs. For Abraxane®, probably the release rate is due to the slow dissociation of the complex formed between albumin and PTX. These results suggest that the drug would be stable in the systemic circulation and it would be released slowly at the tumor site.[32]

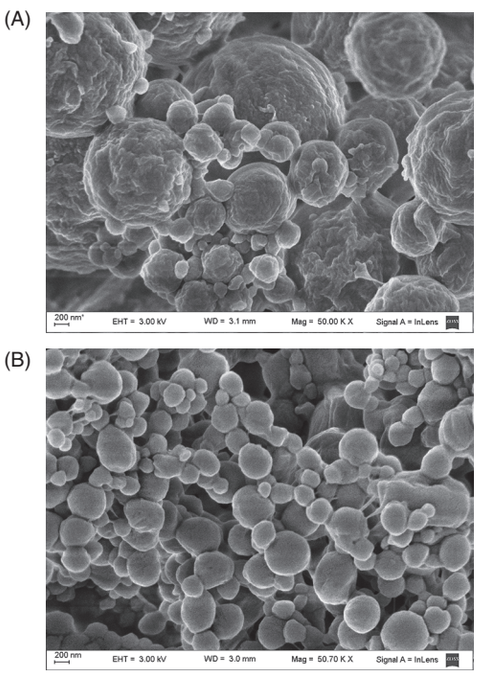

Figure 2. SEM micrographs of PTX-loaded (A) mPEG-*b*-PCL NPs and (B) TPGS-*b*-PCL NPs. Magnification: 50,000×.

3.5. *In Vitro* Citotoxicity

The *in vitro* performance of PTX-loaded NPs was tested in two human breast cancer cell lines: an estrogen-dependent (MCF-7) and an estrogen independent (MDA-MB-231) using the WTS assay for both nanocarrier systems at 48 and 72 h (Figs. 4 and 5). In order to characterize the *in vitro* PTX therapeutic effect, the IC_{50} values were estimated for each system at every incubation timepoint and the results are summarized on Tables II and III. For MCF-7 breast cancer cell line, PTX-loaded TPGS-*b*-PCL NPs exhibited a higher citotoxicity than a PTX solution and the nanosized commercially available formulation (Abraxane®), being this effect more marked as the PTX concentration was increased. Interestingly, TPGS-based NPs also exhibited a higher citotoxicity than its counterpart mPEG-*b*-PCL-based nanocarrier after 48 h and 72 h of incubation (Figs. 4 and 5). This effect could

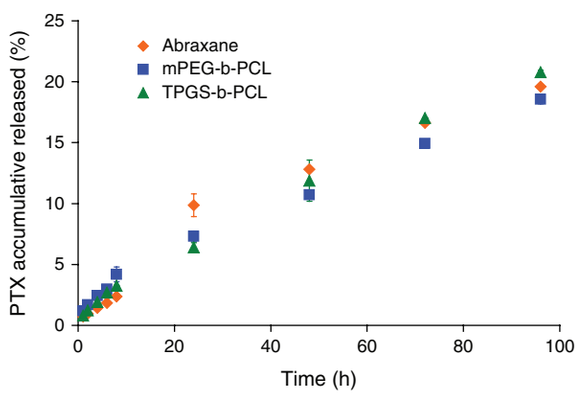

Figure 3. PTX accumulative release profile from mPEG-*b*-PCL NPs and TPGS-*b*-PCL NPs in comparison with Abraxane® at 37 °C over 96 h. Data are expressed as mean ± S.D. ($n = 3$).

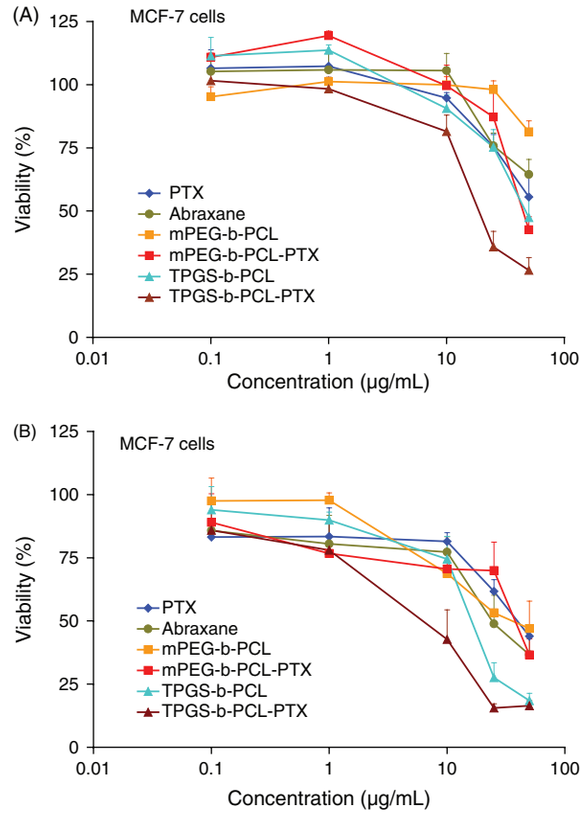

Figure 4. Viability of human breast cancer MCF-7 cells determined by WST assay after (A) 48 h and (B) 72 h of incubation with PTX solution, Abraxane®, PTX-loaded mPEG-*b*-PCL NPs and PTX-loaded TPGS-*b*-PCL NPs, employing the same PTX dose for every assay. Notice that a molar equivalent drug-free mPEG-*b*-PCL NPs and TPGS-*b*-PCL NPs were used. Results are expressed as mean ± S.D. ($n = 3$).

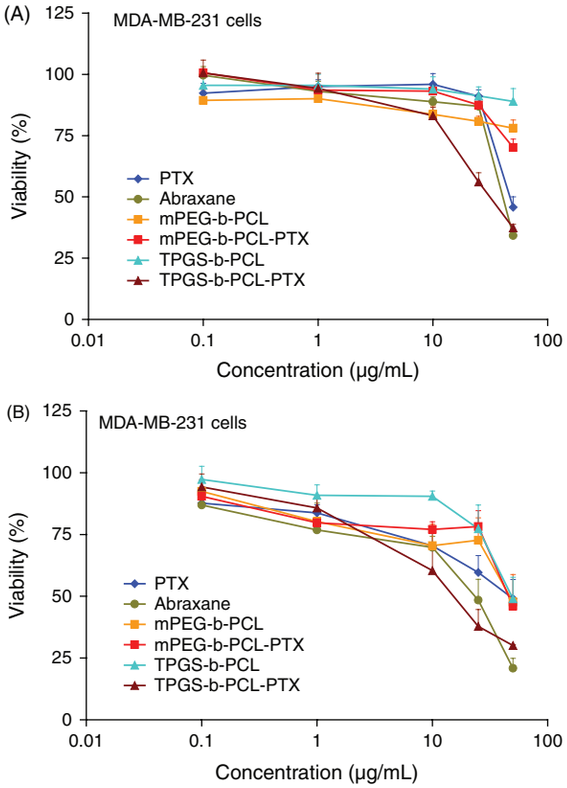

Figure 5. Viability of human breast cancer MDA-MB-231 cells determined by WST assay after (A) 48 h and (B) 72 h of incubation with PTX solution, Abraxane®, PTX-loaded mPEG-*b*-PCL NPs and PTX-loaded TPGS-*b*-PCL NPs, employing the same PTX dose for every assay. Notice that a molar equivalent drug-free mPEG-*b*-PCL NPs and TPGS-*b*-PCL NPs were used. Results are expressed as mean ± S.D. ($n = 3$).

be attributed to the presence of TPGS since it has been demonstrated that this biomaterial exhibits a selective anticancer activity.[33] In addition, the resulting toxicity depends upon a number of factors such as size, concentration and chemical properties.[34] As it is shown on Table II, it was observed a significant ($p < 0.05$) decrease on IC_{50} values from 46.4 μg/mL to 20.1 μg/mL after 48 h of incubation for PTX-loaded mPEG-*b*-PCL and TPGS-*b*-PCL NPs, respectively. These results represent a clear enhancement on the *in vitro* citotoxicity performance for the drug-loaded TPGS-*b*-PCL carrier since a lower PTX concentration is needed to kill the 50% of the cancer cell at a designed time. In case of PTX and Abraxane®, their IC_{50} values could not be determined in this assay because at the higher concentration used (50 μg/mL) the viability was greater than 50%. Similar results have been observed by Zhao et al. using the same cell line and after 48 h of treatment.[35]

A similar trend was observed after 72 h where the IC_{50} values significantly ($p < 0.05$) decrease from 41.7 μg/mL, 24.4 μg/mL and 35.5 μg/mL to 8.7 μg/mL for PTX solution, Abraxane®, drug-loaded mPEG-*b*-PCL NPs and PTX-loaded TPGS-*b*-PCL NPs, respectively (Table III). In this case the increment on citotoxicity activity was 4.8-fold and 2.6-fold for the TPGS-*b*-PCL-based nanocarrier in comparison with PTX solution and Abraxane®, respectively. This indicates that TPGS NP formulation might require a lower drug concentration than the other formulations to achieve the same *in vitro* therapeutic efficacy.

On the other hand, it was also observed that PTX-free NPs based on TPGS exhibited an increased citotoxicity as the copolymer concentration was increased (Figs. 4 and 5). For example, the IC_{50} values showed a significant ($p < 0.05$) decrease from 41.7 μg/mL to 16.4 μg/mL for PTX solution and blank TPGS-based NPs after 72 h of incubation. Moreover there was no significant difference between the IC_{50} values for the drug solution and blank mPEG-*b*-PCL NPs (Table II).

In order to gain a further insight on the *in vitro* performance of our novel TPGS-*b*-PCL NPs, we also evaluated their citotoxicity activity in another breast cancer cell line denoted as MDA-MB-231. Particularly, this cancer cells do not express receptors for estrogen, progesterone and human epidermal growth factor type 2 and they are denoted as a *triple-negative cell line.* Breast tumors of this subtype exhibit poor overall prognosis.[36]

Table II. IC_{50} (mean ± S.D.) values in MCF-7 and MDA-MB-231 cells after 48 h treatment by PTX solution, Abraxane®, blank NPs and PTX-loaded NPs.

	IC_{50} (μg/mL)					
Cell line	PTX	Abraxane®	Blank mPEG-*b*-PCL NPs	PTX-loaded mPEG-*b*-PCL NPs	Blank TPGS-*b*-PCL NPs	PTX-loaded TPGS-*b*-PCL NPs
MCF-7	>50	>50	>50	46.4 ± 0.8	>50	20.1 ± 3.0[a]
MDA-MB-231	47.7 ± 1.5	43.0 ± 0.7	>50	>50	>50	29.7 ± 1.9[b, c]

Notes: Multiple comparisons were performed using one-way ANOVA with Tukey post hoc test ($n = 3$ experiments). [a]Significant difference compared to PTX-loaded mPEG-PCL NPs ($p < 0.05$); [b]significant difference compared to PTX ($p < 0.05$); [c]significantly difference compared to Abraxane® ($p < 0.05$).

For MDA-MB-231 breast cancer cell line, we could only determine the IC_{50} for PTX, Abraxane® and drug-loaded TPGS-*b*-PCL NPs after 48 h of incubation. IC_{50} values of the remaining formulations could not be determined because the cell viability was greater than 50% with the highest concentration used. In this sense, He et al. studied the cytotoxicity against these MDR breast cancer cells line and concentrations of PTX above 100 μg/mL were required for IC_{50} determination.[37] However, PTX-loaded TPGS-*b*-PCL NPs TPGS showed the lowest IC_{50} value (29.7 ± 1.9 μg/mL) at 48 h, being significantly lower than the values for PTX and Abraxane® (Table II). A similar behaviour was observed after at 72 h of incubation where the IC_{50} values decrease from 14.0 μg/mL, 12.1 μg/mL and 26.1 μg/mL to 8.1 μg/mL for PTX solution, Abraxane®, drug-loaded mPEG-*b*-PCL NPs and PTX-loaded TPGS-*b*-PCL NPs, respectively (Table III). In this case, a significant ($p < 0.05$) difference was observed between the drug-loaded nanocarriers. Another interesting point to consider is that TPGS can induce apoptosis in breast cancer cell lines (MCF-7 and MDA-MB-231) but not in "normal" (non-tumorigenic) cells.[38] In our results, the presence of TPGS in the copolymer showed an adjuvant effect with PTX; this effect could enhance the therapeutic activity of different antineoplastic drugs, representing a new concept in the design of drug delivery systems.

Overall, PTX-loaded TPGS-*b*-PCL NPs exhibited a better *in vitro* performance than
(i) its counterpart based on mPEG-*b*-PCL and
(ii) the commercially available Abraxane® for both breast cancer cell lines.

These results could be attribute to two main effects:
(i) the drug encapsulation within the NPs and
(ii) the citotoxic effect display by TPGS.[25]

4. CELLULAR UPTAKE

Previously it has been reported that nanoparticulate systems could enhanced antineoplastic drug uptake by different cancer cell lines.[28, 39, 40] One of the main objectives of the present investigation was the development of a novel nano-sized carrier based on TPGS as a PEG derivative which could improve the PTX accumulation within two breast cancer cell lines. Thereafter the intracellular/cell PTX levels were assessed in MCF-7 and MDA-MB-231 cell lines employing a PTX concentration of 25 μg/mL; according with the IC_{50} values obtained in the *in vitro* citotoxicity assays. As is shown in Figure 6, the PTX uptake is related with the incubation time for the nano-sized carriers. In this case, the longer the incubation time, the grater intracellular PTX concentration, for both cell lines. For TPGS-*b*-PCL NPs it was observed a significant ($p < 0.05$) increase of the intracellular/cell PTX levels in comparison with its counterpart mPEG-*b*-PCL NPs, Abraxane® and PTX solution after 6 h. This translates in an increment of the intracellular/cell PTX concentration of 1.42, 1.85 and 1.6-fold (MCF-7 cell line) and 1.3, 2.18 and 2.32-fold (MDA-MB-231 cell line) for TPGS-*b*-PCL NPs respect to mPEG-*b*-PCL NPs, Abraxane® and PTX solution (Table IV). These results are in line with the *in vitro* citotoxicity assay data since PTX-loaded TPGS-*b*-PCL NPs exhibited the lowest IC_{50} values.

Table III. IC_{50} (mean ± S.D.) values in MCF-7 and MDA-MB-231 cells after 72 h treatment by PTX solution, Abraxane®, blank NPs and PTX-loaded NPs.

	IC_{50} (μg/mL)					
Cell line	PTX	Abraxane®	Blank mPEG-*b*-PCL NPs	PTX-loaded mPEG-*b*-PCL NPs	Blank TPGS-*b*-PCL NPs	PTX-loaded TPGS-*b*-PCL NPs
MCF-7	41.7 ± 5.0	24.4 ± 3.2	33.3 ± 7.8	35.5 ± 9.0	16.4 ± 2.4	8.7 ± 0.7[a, b, c, d, e]
MDA-MB-231	14.0 ± 1.7	12.1 ± 3.8	25.4 ± 8.4	26.1 ± 10.1	39.3 ± 6.1	8.1 ± 2.1[d, e]

Notes: Multiple comparisons were performed using one-way ANOVA with Tukey post hoc test ($n = 3$ experiments). [a]Significant difference compared to PTX ($p < 0.05$); [b]significant difference compared to Abraxane® ($p < 0.05$); [c]significantly difference compared to blank mPEG-PCL NPs ($p < 0.05$); [d]significantly difference compared to PTX-loaded mPEG-PCL NPs ($p < 0.05$); [e]significantly difference compared to blank TPGS-PCL NPs ($p < 0.05$).

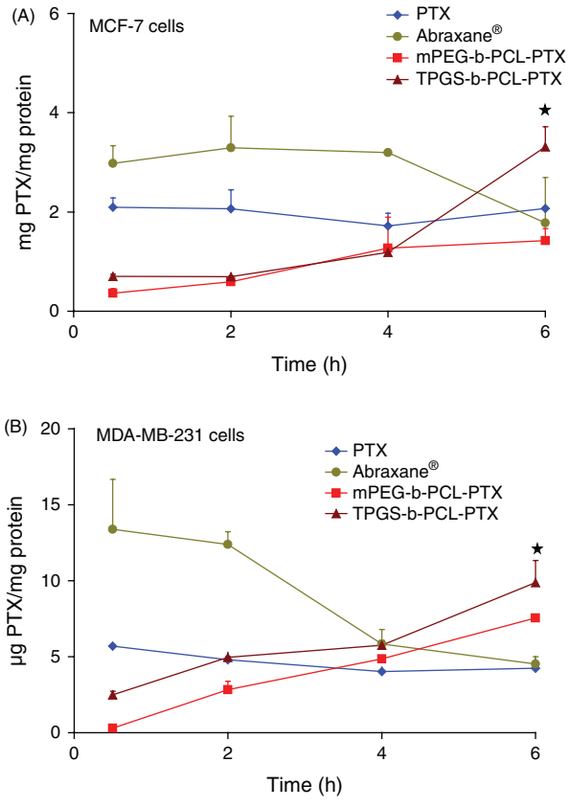

Figure 6. Time-dependent intracellular/cell PTX levels in (A) MCF-7 and (B) MDA-MB-231 breast cancer cell lines for drug-loaded mPEG-*b*-PCL NPs and TPGS-*b*-PCL NPs in comparison with Abraxane® and PTX solution. Drug amount was normalized by protein concentrations of the cell lysates. Results are expressed as mean ± S.D. ($n = 3$). ⋆ The intracellular/cell PTX levels are significantly ($p < 0.05$) higher for TPGS-*b*-PCL NPs in comparison with the other formulations assayed.

Interestingly, for PTX solution the intracellular/cell PTX levels remained almost unchanged over 6 h for MCF-7 cells. Whereas for Abraxane®, drug levels remained almost unchanged only during the first 4 h, then a decrease on PTX values was observed where the drug intracellular/cell concentration between 4 h and 6 h decrease from 3.2 μg/mg to 1.8 μg/mg (Fig 6(A)). In case of MDA-MB-231 cells, there was a clear decrease on the intracellular/cell drug levels for PTX solution and Abraxane®, as is shown on Figure 6(B). For instance, PTX intracellular concentration between 0.5 h and 6 h decrease from 5.70 μg/mg and 13.39 μg/mg to 4.23 μg/mg and 4.52 μg/mg for PTX solution and Abraxane®, respectively. These data could be associated with the PTX efflux from the cancer cell mediated by Multidrug Resistent Protein.[41,42]

5. CELLULAR UPTAKE WITH VERAPAMIL

The decrease on antitumor drug intracellular/cell levels due to the increment of drug efflux by P-gp is a key factor contributing to the development of MDR in cancer cells.[43] Thus, a high expression of P-gp on tumor cells has been correlated with a poor response to PTX treatment and a poor prognosis.[44] Verapamil has been described as a P-gp inhibitor which is able to reverse completely the resistance caused by this efflux pump.[45] In this sense, some breast cancer patients who received PTX with verapamil showed an increase in PTX exposure.[46] Thereafter, an additional PTX cellular uptake assay was performed on MCF-7 and MDA-MB-231 breast cancer cells with the addition of verapamil.

On one hand, as is shown on Figure 7(A), there was no significant increase on PTX uptake for every formulation assayed with verapamil for MCF-7 cells. In this case, in absence of verapamil, the drug intracellular/cell levels were 2.24 μg/mg, 4.51 μg/mg, 1.73 μg/mg and 2.22 μg/mg for PTX solution, Abraxane®, mPEG-*b*-PCL NPs and TPGS-*b*-PCL NPs, respectively. Then, with verapamil, the drug uptake remained almost unchanged with PTX intracellular/cell levels of 2.41 μg/mg, 4.73 μg/mg, 1.46 μg/mg and 1.99 μg/mg for PTX solution, Abraxane®, mPEG-*b*-PCL NPs and TPGS-*b*-PCL NPs, respectively.

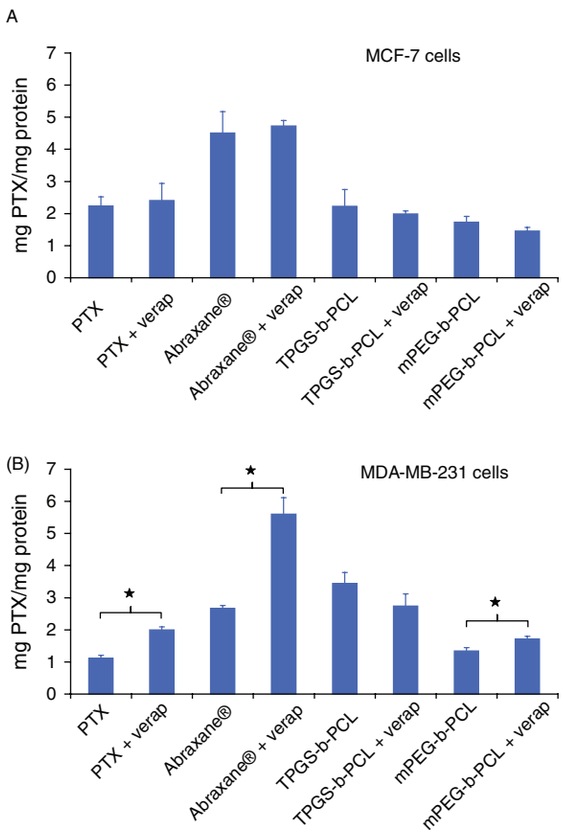

Figure 7. Cellular uptake of PTX from drug solution, Abraxane®, mPEG-*b*-PCL NPs and TPGS-*b*-PCL NPs in absence and presence of verapamil in (A) MCF-7 and (B) MDA-MB-231 breast cancer cell line. PTX amount was normalized by protein concentrations of the cell lysates. Results are expressed as mean ± S.D. ($n = 3$). ⋆ PTX cellular uptake is significantly ($p < 0.05$) different in absence and presence of verapamil.

Therefore, the effect of verapamil on the cellular uptake of PTX was no significant, regardless of incubation time. Similar results have been observed by Baek et al.[47]

On the other hand, a different behavior was observed for MDA-MB-231 cells. Results showed that the uptake of PTX significantly ($p < 0.05$) increased from 1.1 μg/mg to 1.9 μg/mg without and with verapamil for PTX solution (Fig. 7(B)). This result clearly denotes that the drug intracellular/cell levels increased duo to the presence of verapamil. In this context, similar results were expected for Abraxane® and mPEG-*b*-PCL NPs. For instance, the PTX uptake also significantly ($p < 0.05$) increased for both formulations in absence and presence of verapamil for MDA-MB-231 cells (Fig. 7(B)). The PTX intracellular/cell levels increased from 2.66 μg/mg and 1.34 μg/mg to 5.60 μg/mg and 1.71 μg/mg, before and after verapamil addition for Abraxane® and mPEG-*b*-PCL NPs, respectively. Interestingly there was no significant increase on drug uptake for TPGS-*b*-PCL NPs after verapamil incorporation. In this case, the PTX intracellular/cell level was 3.45 μg/mg and 2.74 μg/mg, without and with the presence of verapamil, respectively, denoting the P-gp-inhibiting effect of TPGS.[20]

The different results observed between MCF-7 and MDA-MB-231 cell lines could be explain in terms on Pg-p expression. It has previously described that MDA-MB-231 cells express P-gp, however the MCF-7 cells do not express this transmembrane efflux protein.[46,48] Then, the P-gp-inhibiting effect of verapamil could be clearly observed in MDA-MB-231 where a significant increment on PTX intracellular/cell levels was obtained for TPGS-free formulations. In case of TPGS-*b*-PCL NPs, this PEG-derivate has been also described as a Pg-p inhibitor, and then the inhibition effect of P-gp by verapamil could not be observed. Using a similar strategy with verapamil and other MDR cells, Chavanpatil et al. observed that inhibition of P-gp restores sensitivity to PTX.[49]

6. CONCLUSION

In this work, we prepared two amphiphilic block copolymers with PCL, one decorated with mPEG and another with TPGS to prepare PTX-loaded NPs. Until now, there was not data exhibited the comparison between mPEG-*b*-PCL and TPGS-*b*-PCL copolymers. We observed that TPGS-*b*-PCL NPs presented better antitumoral activity compared to PEG-decorated NPs and the commercial formulation Abraxane® at different concentrations assayed on MCF-7 and MDA-MB-231 breast cancer cells. Also, TPGS-decorated NPs was found to be more effective than the other formulations to internalize PTX in both cell lines. This is the first report comparing the in vitro cytotoxicity and PTX cellular uptake using PEG- and TPGS-decorated NPs. These results showed that TPGS is a more convenient alternative to replace PEG in the nanoparticulate systems used in cancer. Overall, our novel nanosized carrier represents an excellent nanotechnological platform to improve the PTX accumulation within breast cancer cells.

Acknowledgments: Authors thank the University of Buenos Aires (Grant UBACyT 20020100300088 and 20020120200058). Ezequiel Bernabeu and Marcela A. Moretton are supported by postdoctoral scholarship of CONICET, Argentina. Lorena Gonzalez and Diego A. Chiappetta are partially supported by CONICET, Argentina.

References and Notes

1. C. M. Dawidczyk, C. Kim, J. H. Park, L. M. Russell, K. H. Lee, M. G. Pomper, and P. C. Searson, *J. Control. Release* 187, 133 (**2014**).
2. Y. Darren and C. B. Devika, *J. Biomed. Nanotechnol.* 10, 2371 (**2014**).
3. H. S. Nalwa and T. J. Webster (eds.), Cancer Nanotechnology: Nanomaterials for Cancer Diagnosis and Therapy, American Scientific Publishers, Los Angeles, CA (**2008**).
4. Y. Zhao, D. Y. Alakhova, and A. V. Kabanov, *Adv. Drug Deliv. Rev.* 65, 1763 (**2013**).
5. J. Gong, M. Chen, Y. Zheng, S. Wang, and Y. Wang, *J. Control. Release* 159, 312 (**2012**).
6. Z. Gao, L. Zhang, and Y. Sun, *J. Control. Release* 162, 45 (**2012**).
7. A. Karagoz and S. Dincer, *Macromol. Symp.* 295, 131 (**2010**).
8. S. Parveen, R. Misra, and S. K. Sahoo, *Nanomedicine* 8, 147 (**2012**).
9. D. E. Owens III and N. A. Peppas, *Int. J. Pharm.* 307, 93 (**2006**).
10. T. K. Dash and V. Badireenath Konkimalla, *J. Control. Release* 158, 15 (**2012**).
11. M. A. Woodroff and D. W. Hutmacher, *Prog. Polym. Sci.* 35, 1217 (**2010**).
12. P. Aggarwal, J. B. Hall, C. B. McLeland, M. A. Dobrovolskaia, and S. E. McNeil, *Adv. Drug Deliv. Rev.* 61, 428 (**2009**).
13. W.-J. Lin, L.-W. Juang, C.-L. Wang, Y.-C. Chen, C.-C. Lin, and K.-L. Chang, *J. Exp. Clin. Med.* 2, 4 (**2010**).
14. J. Hou, C. Qian, Y. Zhang, and S. Guo, *J. Biomed. Nanotechnol.* 9, 231 (**2013**).
15. G. Gaucher, M.-H. Dufresne, V. P. Sant, N. Kang, D. Maysinger, and J.-C. Leroux, *J. Control. Release* 109, 169 (**2005**).
16. J. M. Harris, N. E. Martin, and M. Modi, *Clin. Pharmacokinet.* 40, 539 (**2001**).
17. S. T. Duggan and G. M. Keating, *Drugs* 71, 2531(**2011**).
18. N. M. Molino, K. Bilotkach, D. A. Fraser, D. Ren, and S.-W. Wang, *Biomacromolecules* 13, 974 (**2012**).
19. G. Ismailos, C. Reppas, and P. Macheras, *Eur. J. Pharm. Sci.* 1, 269 (**1994**).
20. E. Bernabeu and D. A. Chiappetta, *J. Biomater. Tissue Eng.* 3, 122 (**2013**).
21. M. A. Moretton, C. Taira, S. Flor, E. Bernabeu, S. Lucangioli, C. Höcht, and D. A. Chiappetta, *Colloids Surf. B Biointerfaces* (**2014**), in press, DOI: 10.1016/j.colsurfb.2014.09.031.
22. L. Mu and S. S. Feng, *J. Control. Release* 80, 129 (**2002**).
23. M. V. Varma and R. Panchagnula, *Eur. J. Pharm. Sci.* 25, 445 (**2005**).
24. C. M. Neophytou, C. Constantinou, P. Papageorgis, and A. I. Constantinou, *Biochem. Pharmacol.* 89, 31 (**2014**).
25. E. Bernabeu, G. Helguera, M. J. Legaspi, L. Gonzalez, C. Höcht, C. Taira, and D. A. Chiappetta, *Colloids Surf. B Biointerfaces* 113, 43 (**2014**).
26. E. Bernabeu, S. Flor, C. Höcht, C. Taira, D. A. Chiappetta, V. Tripodi, and S. Lucangioli, *Curr. Pharm. Anal.* 8, 185 (**2014**).
27. Y.-J. Wang, C. Wang, C.-Y. Gong, Y.-J. Wang, G. Guo, F. Luo, and Z.-Y. Qian, *Int. J.Pharm.* 434, 1 (**2012**).

28. H.-J. Yao, R.-J. Ju, X.-X. Wang, Y. Zhang, R.-J. Li, Y. Yu, L. Zhang, and W.-L. Lu, *Biomaterials*. 32, 3285 **(2011)**.
29. F. Yan, C. Zhang, Y. Zheng, L. Mei, L. Tang, C. Song, H. Sun, and L. Huang, *Nanomedicine* 6, 170 **(2010)**.
30. F. Lince, D. L. Marchisio, and A. A. Barresi, *J. Colloid Interface Sci.* 322, 505 **(2008)**.
31. Y. Zhang, L. Tang, L. Sun, J. Bao, C. Song, L. Huang, K. Liu, Y. Tian, G. Tian, Z. Li, H. Sun, and L. Mei, *Acta Biomater.* 6, 2045 **(2010)**.
32. T. Yang, F.-D. Cui, M.-K. Choi, J.-W. Cho, S.-J. Chung, C.-K. Shim, and D.-D. Kim, *Int. J. Pharm.* 338, 317 **(2007)**.
33. Y. Guo, J. Luo, S. Tan, B. O. Otieno, and Z. Zhang, *Eur. J. Pharm. Sci.* 49, 175 **(2013)**.
34. Y. L. Zhao and H. S. Nalwa (eds.), Nanotoxicology: Interactions of Nanomaterials with Biological Systems, American Scientific Publishers, Los Angeles, CA **(2007)**.
35. L. Zhao and S. S. Feng, *J. Pharm. Sci.* 99, 3552 **(2010)**.
36. G. Palma, C. Conte, A. Barbieri, S. Bimonte, A. Luciano, D. Rea, F. Ungaro, P. Tirino, F. Quaglia, and C. Arra, *Int. J. Pharm.* 473, 55 **(2014)**.
37. H. He, S. Chen, J. Zhou, Y. Dou, L. Song, L. Che, X. Zhou, X. Chen, Y. Jia, J. Zhang, S. Li, and X. Li, *Biomaterials* 34, 5344 **(2013)**
38. C. M. Neophytou, C. Constantinou, P. Papageorgis, and A. I. Constantinou, *Biochem. Pharmacol.* 89, 31 **(2014)**.
39. J.-H. Park, J.-Y. Lee, U. Termsarasab, I.-S. Yoon, S.-H. Ko, J.-S. Shim, H.-J. Cho, and D.-D. Kim, *Int. J. Pharm.* 473, 426 **(2014)**.
40. K. S. Yadav, S. Jacob, G. Sachdeva, and K. K. Sawant, *J. Nanosci. Nanotechnol.* 11, 6657 **(2011)**.
41. H. Gréen, P. Söderkvist, P. Rosenberg, G. Horvath, and C. Peterson, *Clin. Cancer Res.* 12, 854 **(2006)**.
42. K. Katayama, K. Noguchi, and Y. Sugimoto. *New J. Sci.* **(2014)**, Article ID 476974.
43. R. N. Montesinos, A. Béduneau, Y. Pellequer, and A. Lamprecht, *J. Control. Release* 161, 50 **(2012)**.
44. A. T. Fojo and M. Menefee, *Semin. Oncol.* 32, S3 **(2005)**.
45. M. Huang and G. T. Liu, *Cancer Letters* 135, 97 **(1999)**.
46. S. L. Berg, A. Tolcher, J. A. O'Shaughnessy, A. M. Denicoff, M. Noone, F. P. Ognibene, K. H. Cowan, and F. M. Balis, *J. Clin. Oncol.* 13, 2039 **(1995)**.
47. J.-S. Baek and C.-W. Cho, *J. Pharm. Pharmacol.* 65, 72 **(2012)**.
48. J. Chen, L. Lu, Y. Feng, H. Wang, L. Dai, Y. Li, and P. Zhang, *Cancer Letters* 300, 48 **(2011)**.
49. M. D. Chavanpatil, Y. Patil, and J. Panyam, *Int. J. Pharm.* 320, 150 **(2006)**.

Received: 29 September 2014. Accepted: 12 December 2014.